CrossMark

Relationship between hepatocellular carcinoma circulating tumor cells and tumor volume

Rahmi Oklu[1†], Rahul Sheth[1], Hassan Albadawi[5], Irun Bhan[3,4], A. Fatih Sarioglu[2], Melissa Choz[2,4], Mahnaz Zeinali[2], Vikram Deshpande[6], Shyamala Maheswaran[4,5], Daniel A. Haber[3,4,7], Shannon L. Stott[2,4], Andrew X. Zhu[3,4], Lipika Goyal[3,4], Mehmet Toner[2,5] and David T. Ting[3,4*†] iD

* Correspondence: dting1@mgh.
harvard.edu
†Rahmi Oklu and David T. Ting
contributed equally to this work.
³Department of Medicine,
Massachusetts General Hospital, 55
Fruit St, Boston, MA 02114, USA
⁴Cancer Center, Massachusetts
General Hospital, 149 13th St.,
Charlestown, MA 02129, USA
Full list of author information is
available at the end of the article

Abstract

Background: Microfluidic platforms have demonstrated the ability to isolate rare circulating tumor cells from a wide variety of cancers. Our group has recently shown the ability to isolate circulating tumor cells (CTCs) from hepatocellular carcinoma (HCC) patients using a hematopoietic cell depletion microfluidic platform. However, the relationship of CTC generation and HCC progression is still not well understood. Tumor size is often used as a clinical prognostic factor, but there has been an inconsistent relationship of tumor size and metastatic recurrence. Characterizing the relationship of primary tumor size and CTCs would provide a better understanding of HCC tumor size and metastatic potential.

Results: CTCs in a cohort of HCC patients with quantitative tumor volume analysis was performed to determine if there was a relationship of tumor size to CTC generation. A total of 24 tumor volumetric analyses were used in this study, and a cutoff of 25 cc was used to create a low and high tumor volume group (median 5.56 vs 108 cc; $p < 0.0001$). Using an antigen agnostic microfluidic CTC isolation platform and immunofluorescent staining for cytokeratin and glypican-3, CTCs were detected in 18 of 22 (82%) HCC patients. CTCs/mL of blood did not correlate with either tumor volume or serum AFP. Interestingly, CTCs were found to be significantly higher in small compared to large volume tumors (median 18.5 vs 5 CTCs/mL; $p = 0.0454$).

Conclusion: Altogether, HCC CTCs provide additional data about the tumor independent of standard imaging and blood biomarkers, and there may be biological differences in small volume tumors that facilitate CTC entry into the blood stream. This has implications for HCC CTCs as a biomarker for predicting recurrence and as an early detection platform.

Keywords: Hepatocellular carcinoma, Biomarker, Circulating tumor cells

Background

Hepatocellular carcinoma (HCC) is the second leading cause of cancer mortality worldwide affecting approximately 750,000 patients annually (Stewart & Wild, 2014). Risk factors are well established and include chronic viral hepatitis B and C (HBV and HCV), alcohol use, and non-alcoholic steatohepatitis (NASH). HCC is often diagnosed at a late stage with limited treatment options, and although screening studies have not
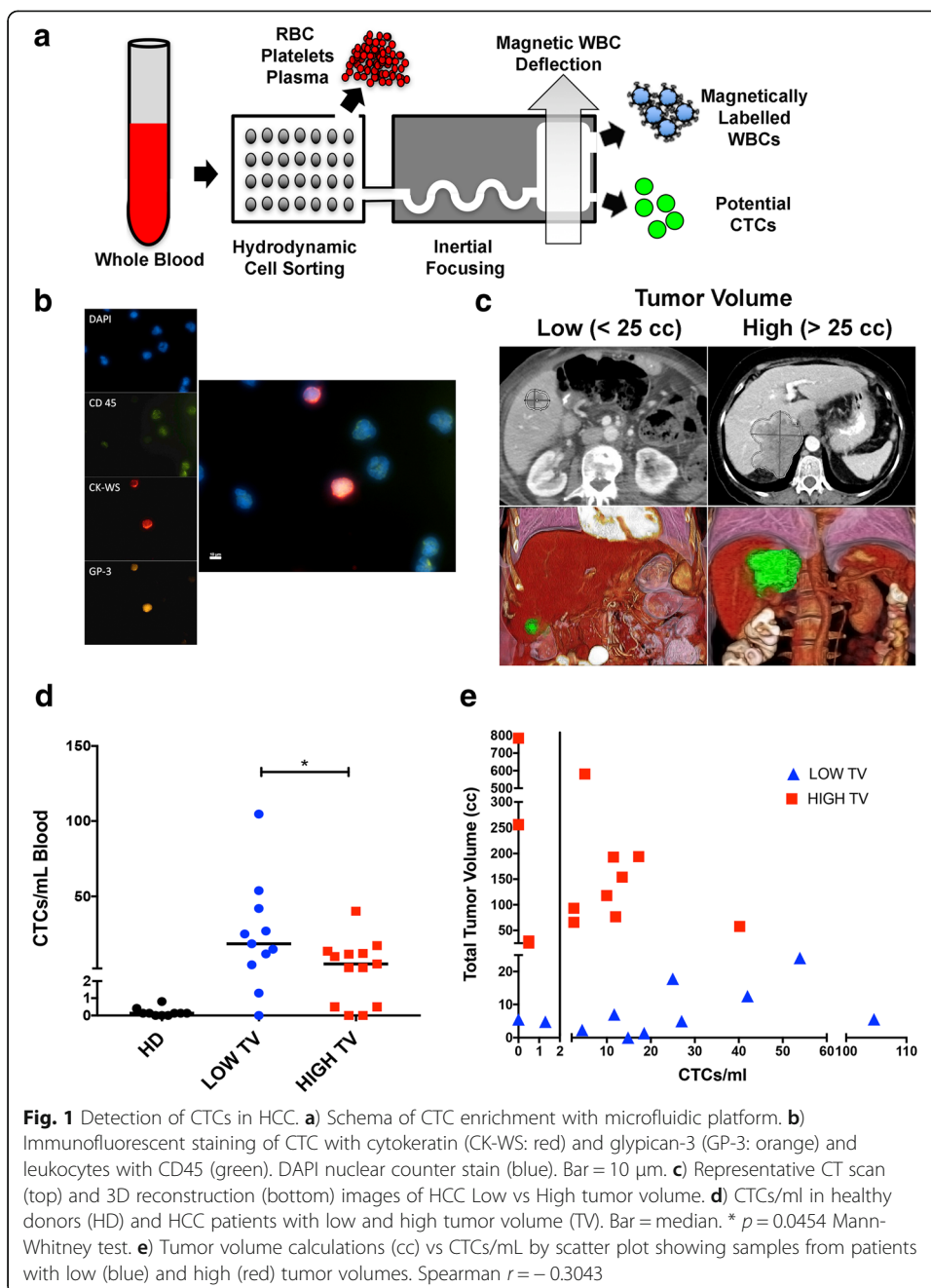
demonstrated a clear mortality benefit, the majority of providers believe that early detection is essential to providing potentially curable therapy (Sherman et al., 2012). The detection of serum AFP has historically been used for HCC surveillance and disease monitoring, but has been shown to be negative in up to 40% of HCC patients making it a suboptimal biomarker (Song et al., 2016). This has led to the use of ultrasound (US) as a primary diagnostic tool for most screening programs with or without AFP testing. However, the sensitivity of US for HCC is as low as 21% for small tumors, and the accuracy of the test is user dependent (Yu et al., 2011a). Given these limitations, the development of novel blood based biomarkers to complement AFP and US is greatly needed for the early diagnosis and monitoring of HCC.

Isolation of circulating tumor cells (CTCs) represent a "liquid biopsy" that can offer a resource to perform a variety of molecular analyses to better understand the biology of HCC as well as serve as a novel blood based diagnostic platform. CTCs have been enriched through a variety of technologies, with the majority utilizing positive CTC antigen capture or size based filtration methods (Yu et al., 2011b). The broadly used Veridex platform utilizing EpCAM positive immunomagnetic enrichment demonstrated 35% and 41% capture rate in two independent HCC studies (Kelley et al., 2015; Sun et al., 2013). This relatively low CTC detection rate is not unexpected given that HCC has the lowest expression level of EpCAM compared to all of the major epithelial cancers as represented in the Cancer Cell Line Encyclopedia (Barretina et al., 2012) (Additional file 1: Figure S1). Given these limitations of positive antigen capture strategies, we employed an antigen agnostic isolation device called the CTC-iChip (Ozkumur et al., 2013) (Fig. 1a). This device uses a combination of hydrodynamic cell sorting to remove small blood products including red blood cells (RBCs), platelets, and plasma with inertial focusing and magnetophoresis of white blood cells (WBCs) to enrich for CTCs that do not have any positive antibody capture bias. We have already demonstrated the ability of the CTC-iChip to enrich for HCC CTCs using a digital drop PCR based RNA signature, which has provided the ability to make binary calls on the presence of CTCs in a blood sample (Kalinich et al., 2017). However, the established immunofluorescent (IF) based enumeration of CTCs affords the ability to quantitate cell numbers, which provides additional insight into the relationship of CTC numbers to tumor progression. The common assumption is that CTC numbers correlate with tumor progression, and therefore, would increase with primary tumor growth. However, it is clear in HCC as well as other tumors that primary tumor size alone is not consistently predictive of metastatic dissemination. We sought to determine if there was a relationship between HCC CTC numbers and tumor size by volumetric imaging analysis, as it has implications for the sensitivity of CTCs to detect early HCC lesions.

Methods

Study enrollment

All clinical studies were approved by the Dana-Farber Harvard Cancer Center (DF/ HCC) Institutional Review Board (Protocol 05–300). Patients were consented and then enrolled prior to blood draws. Upon enrollment, study investigators collected medical data from the patient electronic medical record with patient permission. Disease-free control patients were similarly consented and enrolled. A maximum of 20 ml of blood

Oklu *et al. Cancer Convergence* (2018) 2:2

Page 3 of 9

Fig. 1 Detection of CTCs in HCC. **a**) Schema of CTC enrichment with microfluidic platform. **b**) Immunofluorescent staining of CTC with cytokeratin (CK-WS: red) and glypican-3 (GP-3: orange) and leukocytes with CD45 (green). DAPI nuclear counter stain (blue). Bar = 10 μm. **c**) Representative CT scan (top) and 3D reconstruction (bottom) images of HCC Low vs High tumor volume. **d**) CTCs/ml in healthy donors (HD) and HCC patients with low and high tumor volume (TV). Bar = median. * $p = 0.0454$ Mann-Whitney test. **e**) Tumor volume calculations (cc) vs CTCs/mL by scatter plot showing samples from patients with low (blue) and high (red) tumor volumes. Spearman $r = -0.3043$

was obtained from patients at any given blood draw in two 10-mL EDTA tubes, and approximately 8–10 ml of blood was processed per patient.

Purification of CTCs from whole blood using the CTC-iChip

Prior to running blood through the CTC-iChip, blood was analyzed by a cell blood count machine to determine total WBC count. Biotinylated primary antibodies against anti-human CD45 antibody (clone 2D1, R&D Systems, BAM1430) and anti-human CD66b antibody (Abd Serotec, 80H3) were spiked into whole blood (5–10 mL total volume) at 100 fg/WBC and 37.5 fg/WBC, respectively, and incubated rocking at room

Oklu *et al. Cancer Convergence* (2018) 2:2

Page 4 of 9

temperature for 20 min. Dynabeads MyOne Strepavidin T1 (Life Technologies, 65,602) magnetic beads were then added and incubated rocking at room temperature for an additional 20 min. The total blood volume (5–10 mL) was then run on the CTC-iChip as previously described (Ozkumur et al., 2013). After whole-blood CTC-iChip processing, the product containing enriched cells were fixed with 2% paraformaldehyde for 10 min and then cytospun using a Shandon EZ Megafunnel (ThermoFisher A78710001) at 2000 rpm for 5 min. Megafunnel was allow to sit on benchtop for an additional 10 min. A hydrophobic barrier pen was used around the Megafunnel region on the slide and the slide was washed twice with PBS and stored at 4° C in PBS before staining. Slides were blocked for immunofluorescent (IF) staining using 5% donkey serum + 0.3% Triton-X in PBS for 1 h at RT. Primary antibodies (each at 1:50 dilution in PBS, 0.1% BSA, 0.3% Triton-X) targeting wide spectrum cytokeratin (WS CK antibody – Abcam ab9377), Glypican-3 (GPC3 antibody Abcam ab81263), and CD45 (Becton Dickenson 555,480) were then added and incubated for 1 h at RT. Secondary antibodies (each at 1:200 dilution in PBS, 0.1% BSA, 0.3% Triton-X) directed against each of the primary antibodies were then used for fluorescent labelling: 1) WS CK – donkey anti-rabbit Alexa-647 (Jackson ImmunoResearch 711–605-152); 2) GPC3 – donkey anti-sheep Cy3 (Jackson ImmunoResearch 713–165-003); 3) CD45 – donkey anti-mouse Alexa-488 (Jackson ImmunoResearch 715–545-150), which were incubated for 1 h at RT protected from light. Cell nuclei were counterstained with DAPI (5 μg/ mL in PBS, Life Technologies). Slides were mounted using ProLong Gold Antifade Reagent (Life Technologies). Fixed and stained cells were imaged by fluorescence microscopy (TiE or Eclipse 90i, Nikon) using the appropriate filter cubes for image acquisition and the BioView platform for automated image analysis. All candidate CTCs detected were reviewed and scored based on intact morphology, colocalization of CTC markers (WS CK Alexa-647 and/or GPC3 Cy3) with DAPI nuclear counterstain, and absence of leukocyte markers (CD45 Alexa-488).

Tumor volume calculations

For calculation of tumor volumes, a radiologist with subspecialty training in abdominal imaging analyzed the patient's imaging study (either computed tomography or magnetic resonance imaging) most proximal to the time of circulating tumor cell blood draw. Calculations were done using a standard clinical three-dimensional image analysis software package (iNtuition; TeraRecon, Foster City, CA). To use the software, axial slices ranging in thickness of 1.25 mm were transferred to a 3D workstation, and the radiologist manually identified and outlined the intrahepatic malignant lesions. Then the software package's segmentation analysis tools captured the lesions in three orthogonal planes to accurately reflect the size of lesion. Finally, the software calculated the tumor volumes of the regions of interest.

Statistical methods

Statistical analysis was performed using GraphPad PRISM 7. Statistical methods in Table 1 are described in the footnote. Correlation between tumor volumes, AFP levels, and CTC counts was assessed using the Spearman's rank order coefficient.

Oklu *et al. Cancer Convergence* (2018) 2:2

Page 5 of 9

Table 1 Patient characteristics of Low (< 25 cc) vs High (> 25 cc) tumor burden

	Low tumor burden	High tumor burden	p
Samples/Patients	11/11	13/11	
Age, years (median, [range])	67.3 [43.4–78.9]	70.7 [50.2–82.7]	0.21
Gender (M/F)	10/1	9/2	0.99
ECOG			0.99
0	4	6	
1	4	5	
2	1	2	
3	1	0	
Cause of cirrhosis			0.36
Alcohol	5	2	
HBV/HCV	2	2	
NASH	1	4	
Other	3	3	
Labs at CTC draw (median, [range])			
Total bilirubin, mg/dL	1.0 [0.5–3.7]	0.85 [0.4–2.4]	0.15
Albumin, g/dL	4.1 [3.0–4.9]	3.95 [3.0–4.7]	0.58
Platelets, 10^3/μL	123 [61–208]	200 [69–493]	***0.04***
INR	1.2 [1.0–1.4]	1.1 [0.9–1.4]	0.23
Creatinine, mg/dL	1.00 [0.76–1.29]	0.99 [0.69–1.83]	0.85
AFP, ng/mL	9.1 [1.5–9524]	69 [2.2–132,367]	0.18

Note data for age, ECOG status, and labs were done at the time of CTC analysis
p value < 0.05 considered significant and bold italicized in table
p value for ordinal data (age and labs) were done using the Mann-Whitney test
p value for categorical data was done by Fisher Exact (gender, ECOG, cause of cirrhosis). ECOG 0–1 vs 2–3 and cause of cirrhosis alcohol vs all other causes were compared

Results

To optimize the CTC-iChip for HCC CTC IF enumeration, we spiked whole blood from normal healthy donors with cells from the HCC cell line HepG2. HepG2 cells incubated with the CellTracker Red CMTPX (Molecular Probes) compound allowed identification of the HepG2 cells in the CTC-iChip. There was > 95% HepG2 cell capture rate by the chip confirming the capability of the chip to successfully capture HCC cells. We then optimized an immunofluorescent staining protocol on HepG2 spiked blood samples to identify HCC CTCs using antibodies against both cytokeratin (CK-WS) and glypican-3 (GP-3) combined with our standard anti-CD45 antibody to exclude contaminating leukocytes in the product (Fig. 1b).

We then tested our assay in 10 healthy donors (HD) to establish a baseline for the assay demonstrating all samples with < 1 CTC/mL. Based on this, we chose a baseline cutoff of ≥ 2 CTCs/mL for positive detection and applied the assay on 22 patients with HCC diagnosed by histological confirmation by biopsy (*n* = 17) or established radiological criteria (*n* = 5) (Additional file 2: Table S1). We then performed volumetric analysis of each primary tumor to obtain a more accurate estimation of tumor burden and separated patients into low and high tumor volume cohorts using a cutoff of 25 cc (Fig. 1c). The low compared to high volume tumors had a median volume of 5.56 cc versus 108 cc (Mann-Whitney *p* < 0.0001). Evaluation of other clinical parameters (Table 1: age, gender, ECOG status, cause of cirrhosis, total bilirubin, albumin, platelets, INR, creatinine, AFP) were not significantly different between the two groups with the

Oklu *et al. Cancer Convergence* (2018) 2:2

Page 6 of 9

exception of platelets, which were significantly lower (Mann-Whitney $p = 0.04$) in patients with low (median $123 \times 10^3/\mu L$) compared to high (median $200 \times 10^3/\mu L$) tumor burden.

Blood from each of these patients was analyzed for our liver CTC assay. Note, one patient had 3 separate draws for a total of 24 independent blood samples for analysis. Using these criteria, we detected CTCs from 18 of 22 (82%) HCC patients with 18 of 24 independent samples having a mean and median of 17.4 and 11.6 CTCs/mL, respectively. Surprisingly, we found higher CTCs in low vs high volume tumors (Fig. 1d; median 18.5 vs 5 CTCs/mL; Mann-Whitney $p = 0.0454$). We found no correlation of CTC counts with tumor volume (Fig. 1e; Spearman $r = -0.3043$; two tailed $p = 0.15$). Interestingly, low volume tumors tended to have a positive correlation with CTCs/mL (Spearman $r = 0.49$; two tailed $p = 0.13$), while high volume tumors had a slight negative relationship (Spearman $r = -0.10$; two tailed $p = 0.75$). In patients with very high CTC counts, there were no clear differences in vascular involvement or other imaging features. Comparison of CTC counts with the established HCC marker AFP demonstrated no correlation (Spearman $r = 0.037$; $p = 0.86$). The one patient with serial CTC counts (HCC-016) had the 3rd largest tumor at presentation (256 cc), but interestingly, no detectable CTCs. The patient received proton therapy leading to a significant response in tumor volume (93.2 cc and 29.3 cc at 47 and 111 days from initial CTC collection), but CTC counts became detectable albeit low (2.5 and 0.5 CTCs/mL at 47 and 111 days). The patient had progressive disease 3 months later (202 days from initial CTC collection), and is still currently alive with disease. Another notable patient (HCC-031), had no detectable disease by imaging post-liver transplant for HCC, but had an elevated AFP of 64.9 ng/mL and high CTCs of 14.9 cells/mL. Indeed, this patient later was found to have recurrent HCC by standard imaging 440 days after this CTC analysis. These results indicate that HCC CTCs are providing orthogonal information from tumor volume and AFP levels. As a complementary analysis, 3 patients (HCC-003, 004, 005) had additional blood that was processed in our previously published CTC cluster chip (Sarioglu et al., 2015). Interestingly, all patients had detectable CTC clusters (3– 6.5 CTC clusters/mL) with mixtures of HCC CTCs and normal leukocytes, but all 3 of these patients had small volume tumors (Additional file 3: Figure S2). The detection of these cells in patients without visible disease by imaging and the higher levels of CTCs in small volume tumors suggest that there are biological differences in smaller HCC lesions that enhance entry into circulation.

Discussion

Our study reports approximately double the CTC detection rate compared to the Veridex EpCAM based strategy. Other work with positive capture against the asialoglycoprotein receptor has reported detection as high as 89% (Xu et al., 2011; Li et al., 2014). However, these positive capture strategies often cannot utilize sophisticated methods for the study of CTCs including single cell RNA-sequencing and culturing, which we have demonstrated with the CTC-iChip for a variety of other epithelial cancers (Ting et al., 2014; Yu et al., 2014; Miyamoto et al., 2015; Jordan et al., 2016). Interestingly, our study has revealed the possibility that HCC CTC generation occurs when primary tumors are still relatively small. This suggests that the biology of HCC entry into circulation occurs early in HCC tumorigenesis and that the balance of invasion versus

Oklu *et al. Cancer Convergence* (2018) 2:2

Page 7 of 9

proliferation is important to CTC detection. For example, a very large established HCC with low CTCs may have more proliferative activity, while a smaller HCC with high CTCs has a higher frequency of cells able to invade the circulatory system. This is analogous to microsatellite instability high colorectal tumors, which are often very large, but tend to have a better prognosis given their lower propensity to disseminate. However, entry into circulation likely does not correlate with metastatic potential alone as other attributes are needed to complete the metastatic cascade including survival in the hostile environment of the blood vasculature, extravasation into a distant organ, and the ability to grow in a new microenvironment. This has been shown in our single cell RNA-seq CTC studies where over half of CTCs did not have sufficient RNA for sequencing, and therefore, not viable for metastasis (Ting et al., 2014). We also acknowledge that the use of glypican-3 and cytokeratin does have some limitations in specifically determining the malignant origin of the cells since both of these markers can be found expressed in normal hepatocytes. Therefore, the higher CTCs seen in smaller tumors may also represent a combination of tumor cells and normal epithelial cells reflecting differences in peri-tumoral inflammation leading to shedding of normal hepatocytes. Moreover, CTC clusters were seen in small tumors with patients having prolonged survival indicating that not all CTC clusters are metastatic and that the generation of CTC clusters may not be an active process in early carcinogenesis. These considerations indicate that additional CTC markers to address this heterogeneity will be needed to expand the specificity of the assay for HCC and metastatic potential. Nonetheless, the high detection rate (82%) of CTCs in our cohort of HCC patients provides for a highly sensitive marker of disease. A larger prospective clinical trial will be needed to address the prognostic and predictive utility of these assays, but we have provided the foundation for implementation of this CTC assay into the clinical realm.

Conclusion

This study has demonstrated that the relationship between CTC generation and tumor size are not correlated and that smaller HCC primary tumors may have higher access to the vasculature compared to large established tumors. These data provide new insight into the temporal development of CTCs in the metastatic cascade, which must be accounted for in computational modeling of tumor progression. This provides a basis for using CTCs as a means for the early detection of HCC and highlights the intrinsic heterogeneity of cancer cells in circulation.

Additional files

Additional file 1: EpCAM expression levels from cancer cell lines. (TIF 26207 kb)

Additional file 2: Clinical data and CTC counts from patients on study. (XLSX 38 kb)

Additional file 3: CTC clusters in HCC patients. (TIF 27242 kb)

Oklu *et al. Cancer Convergence* (2018) 2:2

Page 8 of 9

Availability of data and materials
All data is presented in this publication, and additional details regarding methods and materials will be provided upon request.

Author contributions
RO and DTT, planned the experiments; RO, MC, MZ, AFS, performed the experiments; LG, AXZ, VD consented patients and provided clinical data; RO, RS, HA, IB, and DTT, analyzed the data; RO, LG, SM, DAH, SLS, AXZ, MT, DTT, wrote and edited the manuscript. All authors read and approved the final manuscript.

Ethics approval and consent to participate
All clinical studies were approved by the Dana-Farber Harvard Cancer Center (DF/HCC) Institutional Review Board (Protocol 05–300). Patients were all prospectively consented on protocol 05–300 for this project.

Consent for publication
Not Applicable.

Competing interests
There are no conflicts to report for all authors.

Publisher's Note
Springer Nature remains neutral with regard to jurisdictional claims in published maps and institutional affiliations.

Author details
[1]Department of Interventional Radiology, Massachusetts General Hospital, 55 Fruit St., Boston, MA 02114, USA. [2]Center for Engineering in Medicine, School of Electrical and Computer Engineering, Georgia Institute of Technology, Atlanta, GA, USA. [3]Department of Medicine, Massachusetts General Hospital, 55 Fruit St, Boston, MA 02114, USA. [4]Cancer Center, Massachusetts General Hospital, 149 13th St., Charlestown, MA 02129, USA. [5]Department of Surgery, Massachusetts General Hospital, 55 Fruit St., Boston, MA 02114, USA. [6]Department of Pathology, Massachusetts General Hospital, Boston, MA 02114, USA. [7]Howard Hughes Medical Institute, Chevy Chase, MD 20815, USA.

References
Barretina J, Caponigro G, Stransky N, Venkatesan K, Margolin AA, Kim S, et al. The Cancer cell line encyclopedia enables predictive modelling of anticancer drug sensitivity. Nature 2012;483(7391):603–307.

Jordan NV, Bardia A, Wittner BS, Benes C, Ligorio M, Zheng Y, et al. HER2 expression identifies dynamic functional states within circulating breast cancer cells. Nature. 2016;

Kalinich M, Bhan I, Kwan TT, Miyamoto DT, Javaid S, LiCausi JA, et al. An RNA-based signature enables high specificity detection of circulating tumor cells in hepatocellular carcinoma. Proc Natl Acad Sci U S A. 2017;114(5):1123–8.

Kelley RK, Magbanua MJ, Butler TM, Collisson EA, Hwang J, Sidiropoulos N, et al. Circulating tumor cells in hepatocellular carcinoma: a pilot study of detection, enumeration, and next-generation sequencing in cases and controls. BMC Cancer. 2015;15:206.

Li J, Chen L, Zhang X, Zhang Y, Liu H, Sun B, et al. Detection of circulating tumor cells in hepatocellular carcinoma using antibodies against asialoglycoprotein receptor, carbamoyl phosphate synthetase 1 and pan-cytokeratin. PLoS One. 2014;9(4):e96185.

Miyamoto DT, Zheng Y, Wittner BS, Lee RJ, Zhu H, Broderick KT, et al. RNA-Seq of single prostate CTCs implicates noncanonical Wnt signaling in antiandrogen resistance. Science. 2015;349(6254):1351–6.

Ozkumur E, Shah AM, Ciciliano JC, Emmink BL, Miyamoto DT, Brachtel E, et al. Inertial focusing for tumor antigen-dependent and -independent sorting of rare circulating tumor cells. Sci Transl Med 2013;5(179):179ra47.

Sarioglu AF, Aceto N, Kojic N, Donaldson MC, Zeinali M, Hamza B, et al. A microfluidic device for label-free, physical capture of circulating tumor cell clusters. Nat Methods. 2015;12(7):685–91.

Sherman M, Bruix J, Porayko M, Tran T. Screening for hepatocellular carcinoma: the rationale for the American Association for the Study of Liver Diseases recommendations. Hepatology (Baltimore MD). 2012;56(3):793–6.

Song PP, Xia JF, Inagaki Y, Hasegawa K, Sakamoto Y, Kokudo N, et al. Controversies regarding and perspectives on clinical utility of biomarkers in hepatocellular carcinoma. World J Gastroenterol 2016;22(1):262–274.

Stewart BW, Wild C, International Agency for Research on Cancer, World Health Organization. World cancer report 2014. Lyon, France Geneva , Switzerland: International Agency for Research on Cancer WHO press; 2014. Xiv, 630 pages p.

Sun YF, Xu Y, Yang XR, Guo W, Zhang X, Qiu SJ, et al. Circulating stem cell-like epithelial cell adhesion molecule-positive tumor cells indicate poor prognosis of hepatocellular carcinoma after curative resection. Hepatology (Baltimore MD). 2013;57(4):1458–68.

Ting DT, Wittner BS, Ligorio M, Vincent Jordan N, Shah AM, Miyamoto DT, et al. Single-cell RNA sequencing identifies extracellular matrix gene expression by pancreatic circulating tumor cells. Cell Rep. 2014;8(6):1905–18.

Oklu *et al. Cancer Convergence* (2018) 2:2

Page 9 of 9

Xu W, Cao L, Chen L, Li J, Zhang XF, Qian HH, et al. Isolation of circulating tumor cells in patients with hepatocellular carcinoma using a novel cell separation strategy. Clinical cancer research : an official journal of the American Association for Cancer Research. 2011;17(11):3783–93.

Yu M, Bardia A, Aceto N, Bersani F, Madden MW, Donaldson MC, et al. Cancer therapy. Ex vivo culture of circulating breast tumor cells for individualized testing of drug susceptibility. Science. 2014;345(6193):216–20.

Yu M, Stott S, Toner M, Maheswaran S, Haber DA. Circulating tumor cells: approaches to isolation and characterization. J Cell Biol. 2011b;192(3):373–82.

Yu NC, Chaudhari V, Raman SS, Lassman C, Tong MJ, Busuttil RW, et al. CT and MRI improve detection of hepatocellular carcinoma, compared with ultrasound alone, in patients with cirrhosis. Clin Gastroenterol Hepatol 2011a;9(2):161–167.